Available online at www.sciencedirect.com
ScienceDirect
Polymer 47 (2006) 6836–6842
polymer
www.elsevier.com/locate/polymer

Synergistic effect of hyperthermal atomic oxygen beam and vacuum ultraviolet radiation exposures on the mechanical degradation of high-modulus aramid fibers

Lipika Ghosh [a], Mohammad Harris Fadhilah [b], Hiroshi Kinoshita [b], Nobuo Ohmae [b,*]

[a] *Graduate School of Science and Technology, Kobe University, 1-1 Rokkodai, Nada, Kobe, Hyogo 657-8501, Japan*
[b] *Faculty of Engineering, Kobe University, 1-1 Rokkodai, Nada, Kobe, Hyogo 657-8501, Japan*

Received 6 January 2006; received in revised form 3 July 2006; accepted 17 July 2006

Abstract

The synergistic effect of atomic oxygen and vacuum ultraviolet (VUV) radiation exposures was investigated on the mechanical properties of high-modulus aramid fibers. Tensile tests were performed on single fibers. It was found that both tensile strength and Young's modulus decreased significantly due to the simultaneous exposures of atomic oxygen and vacuum ultraviolet radiation. In contrast, the surface of aramid fiber exposed to ultraviolet alone showed no change in tensile strength and Young's modulus. X-ray photoelectron spectroscopy showed that atomic oxygen exposure leads to oxidization and decomposition of amid groups, that only VUV exposure does not change the fiber surface, and that VUV exposure decreased oxidized components on the oxidized fiber surface exposed to atomic oxygen and ultraviolet simultaneously. Scanning electron microscopy revealed that the diameter of the fiber was not influenced so much by atomic oxygen and ultraviolet exposures, but the fiber surface became substantially rougher than the aramid fiber surface exposed to atomic oxygen alone.

Keywords: Atomic oxygen; VUV; Aramid fiber

1. Introduction

There are various space environmental factors such as microgravity, thermal cycling, plasma environment (ions and electrons), ultraviolet radiation, particulate radiation, high-energy charged particles, neutral gas and space debris that interact with materials in low Earth orbit (LEO). Material degradation by atomic oxygen is one of the important concerns for space system operated in LEO for a long duration. In space applications, a variety of polymeric materials have been used. The surface of spacecrafts is typically covered with thermal control materials, consisting of a polymer film to control the temperature of the spacecrafts. Atomic oxygen is the dominant reactive species in LEO so that many polymeric materials were deteriorated by high-energy atomic oxygen collisions [1–3]. Spacecraft surfaces in LEO with altitudes of 200–600 km suffer the bombardment with atomic oxygen with a relative collision energy of about 5 eV, which correspond to the orbital velocity of the spacecraft (8 km/s) and a flux of 10^{13}–10^{16} atoms/cm^2/s. Although the severe surface degradation of many polymeric materials due to atomic oxygen attack has been reported, atomic oxygen reactivity with polymeric materials has been investigated in the last two decades [4–8]. Due to its high-chemical reactivity and high-impinging energy on material surfaces (approximately 5 eV, which is attributed to the orbital velocity of spacecrafts), polymeric materials are directly exposed to atomic oxygen in LEO. However, space environmental effect studies are becoming more and more serious for long-term low-risk missions. But one of the difficulties is its synergistic effect in the space environmental effect studies. A synergistic effect of 172 nm vacuum ultraviolet on atomic oxygen-interaction with polyimide enhanced erosion rate more than 300%

* Corresponding author. Tel./fax: +81 78 803 6111.
E-mail address: ohmae@mech.kobe-u.ac.jp (N. Ohmae).

0032-3861/$ - see front matter © 2006 Elsevier Ltd. All rights reserved.
doi:10.1016/j.polymer.2006.07.029

depending on the ultraviolet intensity even though ultraviolet itself does not give any mass-loss on polyimide [9]. Fibrous materials which are frequently used as reinforcements of composites have not been focused yet as a target material in space environmental effect studies. The reason is that the reinforced fibers are covered by matrix in composite materials and are not directly exposed to atomic oxygen attack. However, aramid fiber is a key material for tether satellite, which connects two satellites with flexible cable and needs synthesized fibers with a high-modulus cable material. Due to its higher mechanical properties, high-modulus aramid fiber is well suited for cable material in tether application. So, aramid fiber is directly exposed to atomic oxygen and other space environmental factors for this application.

In this study, the synergistic effect of hyperthermal atomic oxygen beam and vacuum ultraviolet (VUV) radiation on the mechanical properties of aramid fibers has been investigated. Tensile tests were performed on single filament of aramid fibers. The changes in surface chemical state and surface morphology have also been discussed in this study. To our knowledge, no such results are available in the scientific literature of this field.

2. Experimental details

2.1. Atomic oxygen beam facility

The space environment simulation facility in our laboratory, Kobe University, was used in this study, which can simulate atomic oxygen environment in LEO. The laser detonation atomic oxygen beam source, which was originally designed by Physical Sciences Incorporation (PSI), as a hyperthermal atomic oxygen source was equipped in this facility [8]. The ultraviolet source used in this study was an excimer light source with a wavelength of 172 nm. The excimer light source was attached to the atomic oxygen source chamber. The schematic drawing of the facility is shown in Fig. 1. Detail of the experimental apparatus used in this study was explained elsewhere [9]. The ultimate vacuum pressure of this source was kept at 2×10^{-5} Pa. Hyperthermal broad atomic oxygen beam with kinetic energy of approximately 5 eV was obtained to expose the fiber. The flux of atomic oxygen beam was calculated to be 10^{15} atoms/cm^2/s at the sample position by using a silver-coated quartz crystal microbalance (QCM) [10,11]. The axes of the atomic oxygen beam and the ultraviolet crossed at 90° and the sample was placed at the cross point of the beam axes for simultaneous exposure (see Fig. 1).

High-modulus aramid fibers used in this study were Kevlar® 49 (type 420 dtex; density, 1.44 g/cm^3; molecular weight, approximately 20,000 g/mol manufactured by Toray-Dupont Co., Ltd. Japan). The chemical formula of aramid fiber is $(-NH-C_6H_4-NHCO-C_6H_4-CO-)_n$, where $n = 84$. A randomly selected single-filament specimen was carefully separated from the strand bundle. Then the single filament was mounted on a paper holder. A schematic drawing of the sample fiber and its paper holder was reported in our previous study [12]. In order to minimize filament misalignment and bending effects, the ordinary paper tabs were very thin. This specimen was centered over the tab slot by holding the fiber in one end by a tweezer. The other end of the fiber was fixed to the tab by a small drip of low viscosity adhesive, in this case an ordinary paper glue. Then the other end was fixed. A fiber mounted on a paper holder was then attached to the specimen holder in the apparatus and exposed to both sides by atomic oxygen and ultraviolet simultaneously. After exposure, sample was removed from the apparatus and changes in mechanical and surface properties were measured. The exposure procedure was repeated in order to obtain the atomic oxygen fluences of 1.1×10^{18}, 1.1×10^{19}, 1.1×10^{20}, 1.1×10^{21} atoms/cm^2. Ultraviolet radiation with the intensity of 8.5×10^{-4} W/cm^2 was used with atomic oxygen fluences together in every step for the simultaneous exposures.

2.2. Tensile testing

The mechanical properties of the aramid fibers were determined by performing the tensile tests on single fiber. The tests were performed at Murata Machinery, Ltd. in Kyoto, Japan, in an apparatus made by Shimadzu Co., Kyoto, model AG-10kN I.

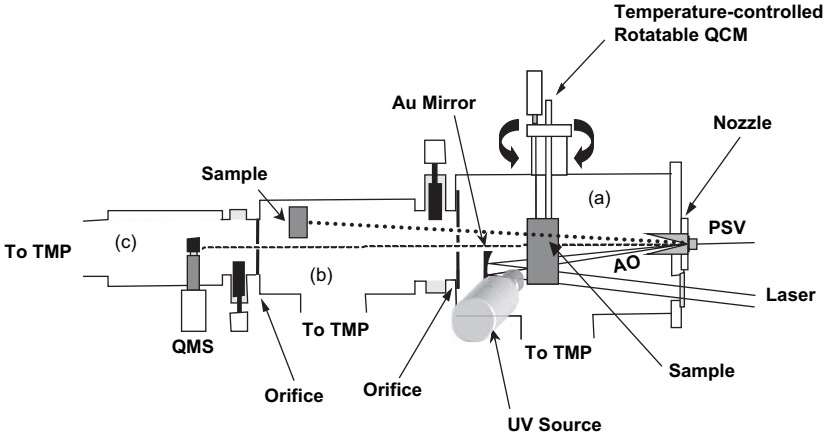

Fig. 1. A schematic drawing of the space environmental simulation facility using a laser detonation atomic oxygen beam source; (a) atomic oxygen source chamber, (b) reaction chamber, (c) time of flight (TOF) chamber. QCM and ultraviolet (UV) sources were attached to the atomic oxygen source chamber.

The system compliance has to be determined in order to obtain accurate measurements. The system compliance was measured by the tensile tests on high-modulus aramid fibers with six different gage lengths. The measurement of system compliance was explained in detail elsewhere [12]. The value of system compliance, Cs, of high-modulus aramid fiber was measured to be 0.3 mm/N at zero gage length. The tensile test was performed according to the ASTM standard for high-modulus single-filament materials, designation D3379-75, edition 1987. The specimen was loaded at a constant crosshead speed of 1 mm/min, while force and displacement were recorded. The tensile test was repeated by 60 measurements on each single filament. Then the average value was taken in order to calculate the tensile strength and Young's modulus of aramid fiber for each data point. Tensile strength was calculated from the maximum load and average cross-sectional area. Young's modulus was calculated from the chart as described in the ASTM standard: Young's modulus = gage length/area (Ca − Cs), where Ca is an apparent compliance which is obtained from the recorded chart and Cs is the system compliance as described earlier.

2.3. Analyses of surface properties

The surface morphology of aramid fibers was observed using a scanning electron microscope (SEM) (JSM-5300). The diameter of the fiber was determined by SEM observations. The average diameter of single filament was measured to be 12.5 μm. The surface chemical composition of atomic oxygen and ultraviolet-exposed aramid fibers was analyzed by X-ray photoelectron spectroscopy (XPS) (ESCA 5400 LS, Perkin–Elmer). The XPS data were collected using a non-monochromated Mg Kα X-ray source (1253.6 eV) and the pressure inside the chamber was held below 1.0×10^{-9} Torr. The XPS spectra were deconvoluted using Gaussian–Lorentzian functions after subtracting background by Shirley's method [13].

3. Results and discussion

It is necessary to confirm whether or not VUV radiation exposure alone affects the tensile strength and Young's modulus of aramid fibers before the simultaneous exposure test of atomic oxygen and VUV. The sample was exposed to ultraviolet radiation with the intensity of 8.5×10^{-4} W/cm^2. The results for the tensile strength and Young's modulus after ultraviolet exposures are shown in Figs. 2 and 3. Obviously, no changes in tensile strength and Young's modulus were observed due to ultraviolet exposure. These experimental results clearly indicate that the ultraviolet radiation with the intensity of 8.5×10^{-4} W/cm^2 does not affect the tensile strength and Young's modulus of aramid fiber. The changes in tensile strength and Young's modulus of the fiber after only atomic oxygen exposure and the simultaneous exposures of atomic oxygen and ultraviolet radiation are shown in Figs. 4 and 5. It was observed that the tensile strength of the fiber decreased from 3.1 GPa to 1.6 GPa (52% of the original value) due to the simultaneous exposures of atomic oxygen and ultraviolet radiation. The decrease in tensile strength of the

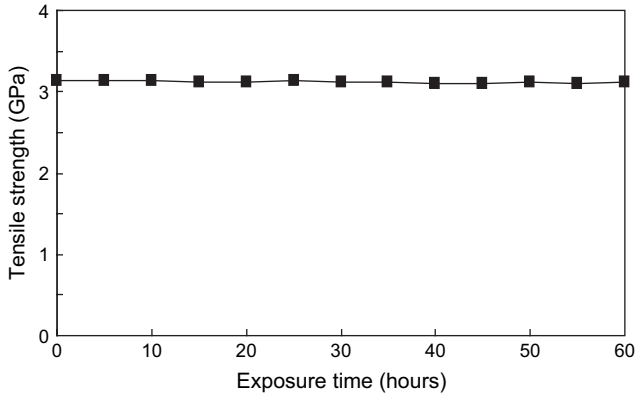

Fig. 2. Change in tensile strength of the high-modulus aramid fibers during ultraviolet exposures. Ultraviolet intensity: 8.5×10^{-4} W/cm^2.

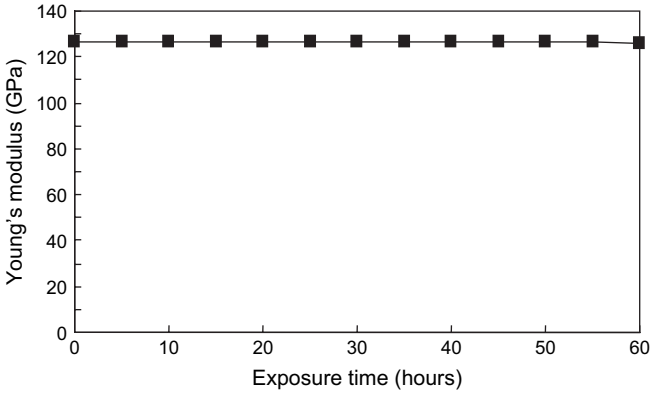

Fig. 3. Change in Young's modulus of the high-modulus aramid fibers during ultraviolet exposures. Ultraviolet intensity: 8.5×10^{-4} W/cm^2.

fiber under simultaneous exposures of atomic oxygen and ultraviolet radiation enhanced 16% to that under atomic oxygen exposure alone. Young's modulus of the fiber also decreased significantly. It decreased from 126.5 GPa to 51.4 GPa (41% of the original value) which observed that the decrease in

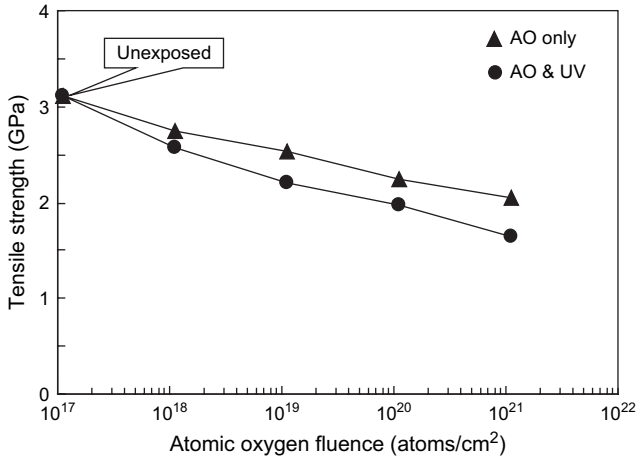

Fig. 4. Tensile strength of the high-modulus aramid fibers under only atomic oxygen exposure and simultaneous exposures of atomic oxygen and ultraviolet radiation. Atomic oxygen flux: 10^{15} atoms/cm^2/s, ultraviolet intensity: 8.5×10^{-4} W/cm^2.

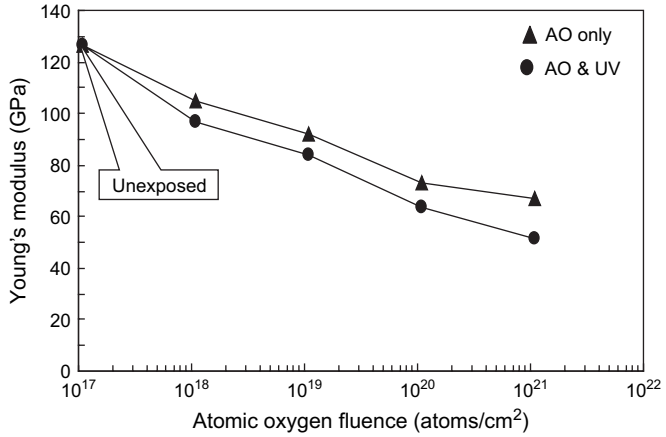

Fig. 5. Young's modulus of the high-modulus aramid fibers exposed to atomic oxygen without and with ultraviolet radiation. Atomic oxygen flux: 10^{15} atoms/cm^2/s, ultraviolet intensity: 8.5×10^{-4} W/cm^2.

Young's modulus of the fiber enhanced 12% under simultaneous exposures of atomic oxygen and ultraviolet radiation to that under atomic oxygen exposure alone. These experimental results suggested that the decrease in tensile strength and Young's modulus is enhanced by the simultaneous ultraviolet exposure. Atomic oxygen- and ultraviolet-exposed fibers were analyzed individually and simultaneously in order to clarify the degradation mechanism on the mechanical properties of aramid fiber due to the simultaneous exposures of atomic oxygen and ultraviolet radiation. SEM images of aramid fibers before and after the atomic oxygen and ultraviolet exposures are shown in Fig. 6. SEM image revealed that the diameter of the fiber was not influenced so much by the atomic oxygen and VUV exposures, even though the fiber surface became substantially rougher (Fig. 6(d)) than the aramid fiber surface exposed to atomic oxygen alone (Fig. 6(c)). On the other hand, ultraviolet-exposed fiber showed no roughness creation on the surface (Fig. 6(b)). The surface chemical composition of aramid fibers analyzed by XPS is presented in Table 1. It was shown that the surface oxygen concentration which was increased to 32.4% due to atomic oxygen exposure, decreased to 28.9% by the simultaneous exposures of atomic oxygen and ultraviolet radiation. The XPS data of the VUV-exposed fiber without atomic

Table 1
Results for the chemical compositions of aramid fibers

Samples	at.%		
	C	O	O/C ratio
Unexposed	85.5	14.5	0.17
AO exposed[a]	67.6	32.4	0.48
UV exposed[b]	85.7	14.3	0.17
AO[a] & UV exposed[b]	71.1	28.9	0.41

[a] AO fluence: 1.1×10^{21} atoms/cm^2.
[b] UV intensity: 8.5×10^{-4} W/cm^2 for 60 h.

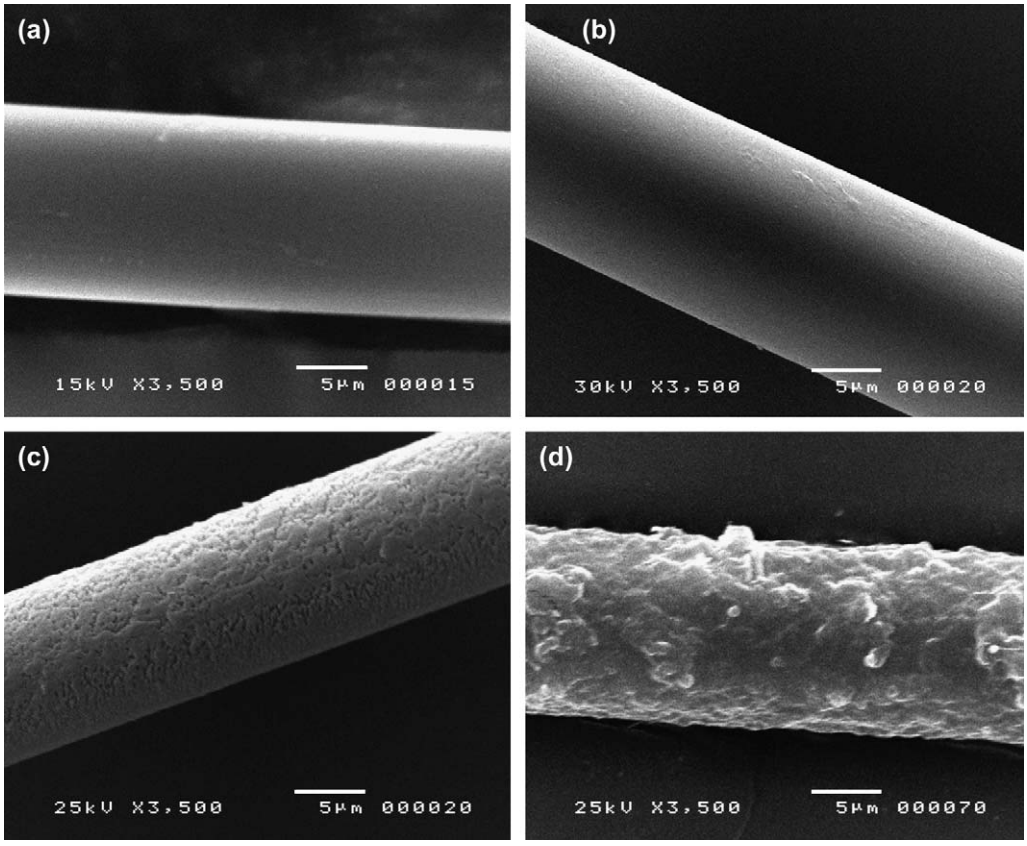

Fig. 6. SEM micrographs of the high-modulus aramid fibers; (a) before exposure, (b) after only ultraviolet exposure of 8.5×10^{-4} W/cm^2 for 60 h, (c) after only atomic oxygen exposure of 1.1×10^{21} atoms/cm^2, (d) after simultaneous exposures of atomic oxygen and ultraviolet (atomic oxygen fluence: 1.1×10^{21} atoms/cm^2, ultraviolet intensity: 8.5×10^{-4} W/cm^2).

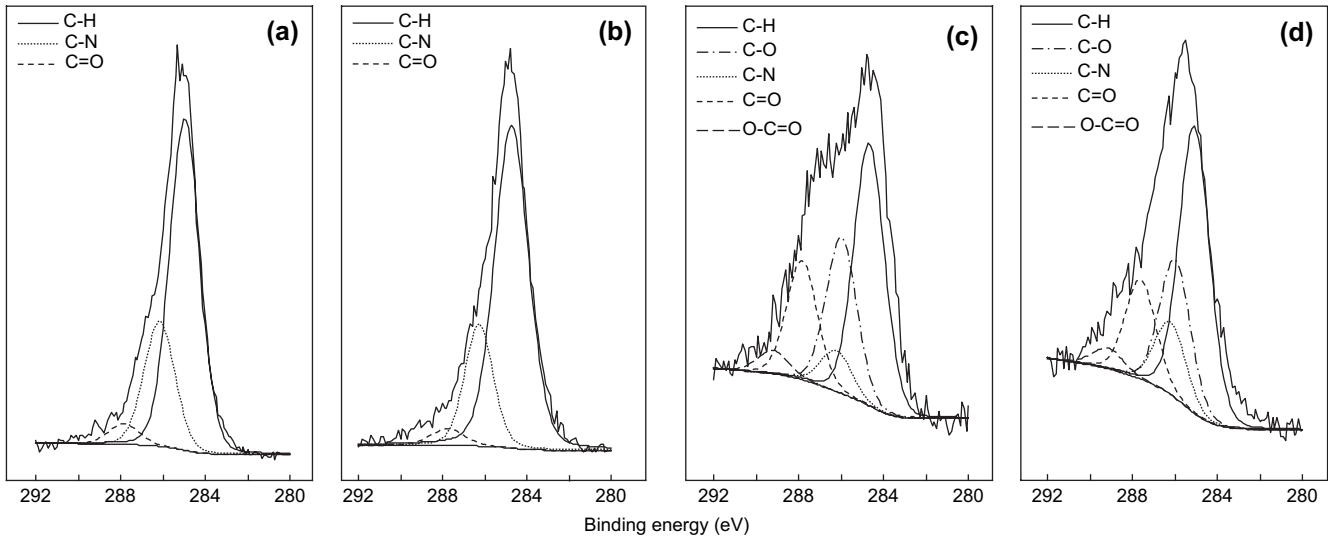

Fig. 7. High-resolution C_{1s} XPS spectra of the high-modulus aramid fibers; (a) before exposure, (b) after ultraviolet exposure of 8.5×10^{-4} W/cm^2 for 60 h, (c) after atomic oxygen exposure of 1.1×10^{21} atoms/cm^2, (d) after simultaneous exposures of atomic oxygen and ultraviolet (atomic oxygen fluence: 1.1×10^{21} atoms/cm^2, ultraviolet intensity: 8.5×10^{-4} W/cm^2).

oxygen exposure are almost identical to that of unexposed fiber as shown in Table 1. It is thus evident that on the oxidized surface by atomic oxygen exposure, VUV exposure leads to desorption of surface oxygen. This result agrees to that of polyimide reported by Brezini and Zekri [14] and Yokota et al. [9,15]. The chemical state of surface oxygen atom was analyzed by high-resolution C_{1s} XPS core-level spectra. Fig. 7 shows C_{1s} photoelectron spectra of aramid fibers before and after atomic oxygen and ultraviolet exposures. Peaks at 284.7, 285.9, 286.2, 287.8 and 289.2 eV correspond to C–H, C–O, C–N, C=O and O–C=O groups, respectively [13]. Results of peak deconvolution are presented in Table 2. It was observed that C–O, C=O and O–C=O components are increased due to atomic oxygen exposure alone. As compared to the only atomic oxygen exposure, the oxidized components were decreased by the simultaneous atomic oxygen and VUV exposures. This result indicates that atomic oxygen exposure results in oxidizing the surface of aramid fiber and decomposition of amid groups, and that in the simultaneous exposure conditions, ultraviolet exposure leads to the decrease in the oxidized components by forming volatile reaction products such as CO or CO_2. The formation of volatile products was detected by atomic oxygen exposure and the similar erosion mechanism for polyimide was reported in literature [9]. The structure of aramid fiber is inhomogeneous in the cross-section and aramid chains are aligned in the peripheral region along with the fiber axis. The structure of aramid fiber was reported in detail elsewhere [16]. The mechanical properties of aramid fiber are attributed to the aligned plates of polymer chains at the peripheral region. Thus, the erosion or distortion of aligned plate in the peripheral region explains the degradation of mechanical properties due to the simultaneous exposures of atomic oxygen and ultraviolet radiation.

Table 2
Surface functional groups distribution of aramid fibers obtained by XPS measurements

Samples	Peak assignments (at.%)				
	C–H	C–O	C–N	C=O	O–C=O
Unexposed	72.2		24.4	3.4	
AO exposed[a]	43.6	26.0	6.7	19.8	3.9
UV exposed[b]	72.4		23.9	3.7	
AO[a] & UV exposed[b]	47.2	22.6	10.8	17.1	2.3

[a] AO fluence: 1.1×10^{21} atoms/cm^2.
[b] UV intensity: 8.5×10^{-4} W/cm^2 for 60 h.

SEM images of atomic oxygen- and ultraviolet-exposed aramid fibers after tensile tests are shown in Fig. 8. Fig. 8(a) and (b) shows the SEM image of the unexposed sample, and Fig. 8(c) and (d) the exposed one under simultaneous exposures of atomic oxygen and ultraviolet (atomic oxygen fluence: 1.1×10^{21} atoms/cm^2, ultraviolet intensity: 8.5×10^{-4} W/cm^2) after tensile tests. It was observed that the unexposed fiber surface shows no crack propagation after tensile tests. In contrast, the exposed fiber shows the lateral cracks propagated along with fiber axis (Fig. 8(c)). Many other cracks were also observed at other positions of the same fiber surface (Fig. 8(d)). This experimental finding revealed that the decrease in tensile strength can be explained by the surface defects such as large cracks introduced into the fiber during atomic oxygen and VUV exposures.

From a series of experiments reported previously, we concluded that the decrease in mechanical properties of aramid fiber due to atomic oxygen exposure can be explained as follows: when aramid fiber surface is exposed to atomic oxygen, the oxidation reaction occurs at the fiber surface. The impinging atomic oxygen is chemically absorbed on the surface and forms oxides, namely carbonyl and carboxyl groups. The oxidized surface then provides atomic oxygen collision-induced production of CO or CO_2 which came from the carbonyl and carboxyl groups. Removal of volatile products from the surface leads to erosion of the peripheral region of

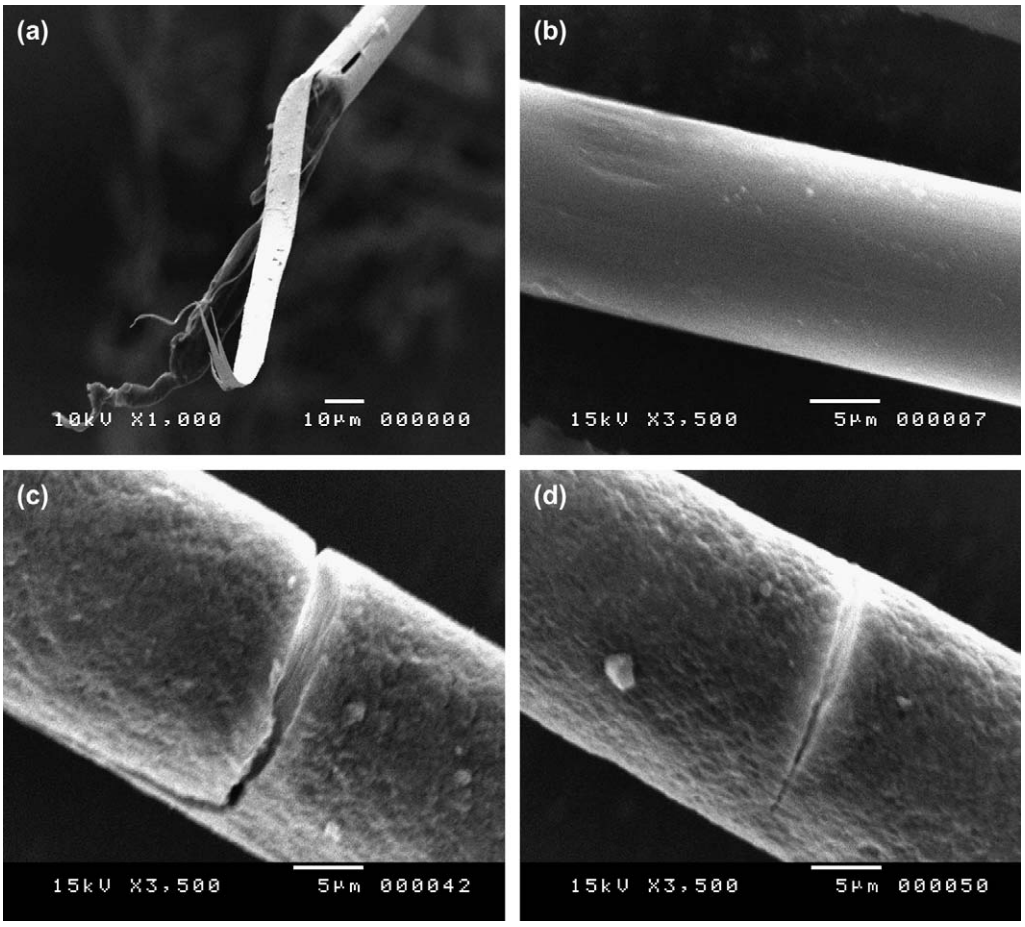

Fig. 8. SEM micrographs of the high-modulus aramid fibers after tensile test; (a) and (b) before exposure, (c) and (d) after simultaneous exposures of atomic oxygen and ultraviolet (atomic oxygen fluence: 1.1×10^{21} atoms/cm^2, ultraviolet intensity: 8.5×10^{-4} W/cm^2).

the fiber and creates rough surface. Crack propagation on the fiber surface governs the decrease in tensile strength of the fiber introduced by atomic oxygen and ultraviolet exposures.

The role of ultraviolet is to boost the gasification reaction during the simultaneous exposures of atomic oxygen and ultraviolet radiation. Ultraviolet exposure does not change tensile strength and Young's modulus of aramid fiber by itself; however, desorption of embedded CO or CO_2 is promoted by ultraviolet exposure. The effect of ultraviolet on the mechanical properties was confirmed in this experiment when the simultaneous exposures under atomic oxygen and ultraviolet enhanced the decrease in tensile strength and Young's modulus of aramid fiber to 16% and 12% more, respectively, than those in the atomic oxygen-exposed surface alone.

4. Conclusions

The synergistic effect of atomic oxygen and VUV radiation exposures was investigated on the mechanical properties of high-modulus aramid fibers. The results of the tensile tests showed that the surface of aramid fiber exposed to ultraviolet alone showed no change in tensile strength and Young's modulus. In simultaneous atomic oxygen and ultraviolet exposure conditions, ultraviolet enhanced the decrease in tensile strength and Young's modulus of aramid fibers to 16% and 12% more, respectively, compared with those in the atomic oxygen-exposed surface alone. It was confirmed that the ultraviolet exposure degraded the mechanical properties of aramid fibers. From the XPS measurements, atomic oxygen exposure results in oxidization and decomposition of amid groups, indicating that the fiber surface was eroded in the peripheral region of aramid fiber. VUV exposure increased the erosion of the fiber surface by forming the gasification reaction. SEM measurements showed that surface of the exposed fiber by atomic oxygen and ultraviolet exposures became substantially rougher than the aramid fiber surface exposed to atomic oxygen alone. The largest crack introduced in the fiber surface which governs the decrease in tensile strength of aramid fiber due to the simultaneous exposures of atomic oxygen and ultraviolet radiation.

Acknowledgements

The authors wish to thank Messrs. N. Yokoi and H. Asada of Kobe University for their help with experiment. We gratefully acknowledge Messrs. Y. Akiyama, Y. Hata, and M. Furukawa of Murata Machinery, Ltd., where all the tensile tests were carried out.

References

[1] Tagawa M, Yokota K, Ohmae N, Kinoshita H. High Performance Polymers 2000;12(1):53–63.

[2] Kinoshita H, Tagawa M, Umeno M, Ohmae N. Surface Science 1999; 440(1):49–59.

[3] Kleiman JI, Gudimenko YI, Iskanderova ZA, Tennyson RC, Morison WD, McIntyre MS, et al. Surface and Interface Analysis 1995;23:335–41.

[4] Minton TK, Garton DJ. Chemical dynamics in extreme environments – advanced series in physical chemistry. Singapore: World Scientific; 2000. p. 420.

[5] Koontz SL, Albyn K, Leger J. Journal of Spacecraft and Rockets 1991; 28(3):315–23.

[6] Golub MA, Wydeven T, Cormia RD. Polymer Communication 1988; 29(10):285–8.

[7] Whitaker AF, Jang BZ. Journal of Applied Polymer Science 1993; 48:1341–67.

[8] Caledonia GE, Krech RH, Green DB. AIAA Journal 1987;25(1):59–63.

[9] Yokota K, Ohmae N, Tagawa M. High Performance Polymers 2004; 16:221–34.

[10] Matijasevic V, Gawin EL, Hammond RH. Review of Scientific Instruments 1990;61:1747–9.

[11] Schumitt A, Offermann EL, Anton R. Thin Solid Films 1996;281:105–7.

[12] Stark AK, Berglund LA, Tagawa M, Ohmae N. Carbon 1994;32(4): 641–4.

[13] Beamson G, Briggs D. Handbook of high resolution XPS organic polymers – the scienta ESCA300 database. Chichester (England): John Wiley & Sons; 1992 [chapter 15].

[14] Brezini A, Zekri N. Journal of Applied Physics 1994;75:2015–25.

[15] Yokota K, Tagawa M, Ohmae N, Kinoshita H. Books of abstracts of 44th space technology and science conference, Fukuoka (Japan); 2000. p. 198 [in Japanese].

[16] Dobb MG, Johnson DJ, Saville BP. Journal of Polymer Science Polymer Physics Edition 1977;15:2201–11.